Link sito dell'editore: https://onlinelibrary.wiley.com/journal/16163028**Link codice DOI**: DOI: 10.1002/adfm.201603023

Citazione bibliografica dell'articolo:

Giuri, A., Masi, S., Colella, S., Kovtun, A., Dell-Elce, S., Treossi, E., Liscio, A., **Corcione, C.E.**, Rizzo, A., Listorti, A. Cooperative Effect of GO and Glucose on PEDOT: PSS for High V OC and Hysteresis-Free Solution-Processed Perovskite Solar Cells **(Adv. Funct. Mater., (2016), 38, (6985), 10.1002/adfm.201603023) (2017) Advanced Functional Materials**, 27 (2), art. no. 17700 11.

Full Paper

xxxx

A. Giuri, S. Masi, S. Colella, A. Kovtun, S. Dell'Elce, E. Treossi, A. Liscio, C. Esposito Corcione, A. Rizzo,* A. Listorti

.....x–xx

Cooperative Effect of GO and Glucose on PEDOT:PSS for High V_{OC} and Hysteresis-Free Solution Processed Perovskite Solar Cells

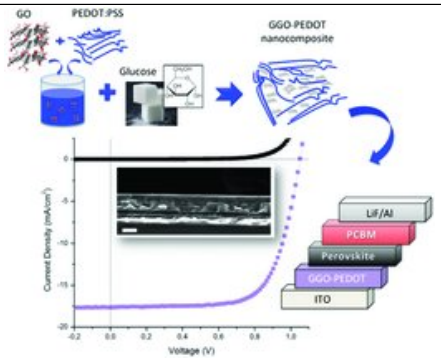

The synergic effect of graphene oxide and glucose in improving the conduction properties of polymer electrolyte poly(3,4-ethylenedioxythiophene):poly(styrenesulfonate) and modifying the sensible interface of perovskite solar cells is reported. This method allows obtaining hysteresis-free and high V_{OC} $CH_3NH_3PbI_3$ devices displaying a ≈37% improvement in power conversion efficiency, evidencing minimal recombination losses and very efficient charge extraction at the electrodes.

Cooperative Effect of GO and Glucose on PEDOT:PSS for High V_{OC} and Hysteresis-Free Solution Processed Perovskite Solar Cells

+ *By Antonella Giuri[1], Sofia Masi[2,3,4], Silvia Colella[2,4], Alessandro Kovtun[5], Simone Dell'Elce[5], Emanuele Treossi[5], Andrea Liscio[5], Carola Esposito Corcione[1], Aurora Rizzo[4,*] and Andrea Listorti[2,4]*

+[1] A. Giuri, Dr. C. Esposito Corcione, Dipartimento di Ingegneria dell'Innovazione, Università del Salento, Via per Monteroni, km 1, 73100, Lecce, Italy

+[2] S. Masi, Dr. S. Colella, Dr. A. Listorti, Dipartimento di Matematica e Fisica "E. De Giorgi,", Università del Salento, Via Arnesano SNC, 73100, Lecce, Italy

+[3] S. Masi, Center for Biomolecular Nanotechnologies (CBN) – Fondazione Istituto Italiano di Tecnologia,, Via Barsanti 14, 73010, Arnesano (Lecce), Italy +Affiliation

+[4] S. Masi, Dr. S. Colella, Dr. A. Rizzo, Dr. A. Listorti, Istituto di Nanotecnologia CNR-Nanotec, Polo di Nanotecnologia c/o Campus Ecotekne, Via Monteroni, 73100, Lecce, Italy +Affiliation

+[5] A. Kovtun, S. Dell'Elce, Dr. E. Treossi, Dr. A. Liscio, Istituto per la Sintesi e la Fotoreattività CNR-ISOF, Via Gobetti 101, 40129, Bologna, Italy +Affiliation

Correspondence to: Dr. A. Rizzo (E-mail: aurora.rizzo@nanotec.cnr.it) Q1: [APT to AU] Please provide the highest academic title (either Dr. or Prof.) for all authors, where applicable. [Reply by AU] ok

Received: 2016-06-17, Online: YYYY-MM-DD

+TITLE

Hybrid organic–inorganic halide perovskites have emerged at the forefront of solution-processable photovoltaic devices. Being the perovskite precursor mixture a complex equilibrium of species, it is very difficult to predict/control their interactions with different substrates, thus the final film properties and device performances. Here the wettability of $CH_3NH_3PbI_3$ ($MAPbI_3$) onto poly(3,4-ethylenedioxythiophene):poly(styrenesulfonate) (PEDOT:PSS) hole transporting layer is improved by exploiting the cooperative effect of graphene oxide (GO) and glucose inclusion. The glucose, in addition, triggers the reduction of GO, enhancing the conductivity of the PEDOT:PSS+GO+glucose based nanocomposite. The relevance of this approach toward photovoltaic applications is demonstrated by fabricating a hysteresis-free $MAPbI_3$ solar cells displaying a ≈37% improvement in power conversion efficiency if compared to a device grown onto pristine PEDOT:PSS. Most importantly, V_{OC} reaches values over 1.05 V that are among the highest ever reported for PEDOT:PSS p-i-n device architecture, suggesting minimal recombination losses, high hole-selectivity, and reduced trap density at the PEDOT:PSS along with optimized $MAPbI_3$ coverage.

Keywords

+ glucose, graphene oxide reduction, PEDOT:PSS nanocomposite, perovskite solar cells, wettability

1 Introduction

Hybrid halide perovskites based solar cells hold promises for low-cost production of highly efficient devices.[1] The versatility of the material facilitates the realization of very different solar cell layouts,[2,3] spanning from mesostructured to planar heterojunction (PHJ) architectures.[4,5,6,7] The extraordinary flourishing of efficient perovskite solar cells witnessed the expected appearance of newcomer drawbacks such as material/device stability and reproducibility.[8,9,10,11] Nevertheless, one of the most disconcerting limitations has been associated to the presence of hysteresis in the photovoltaic behavior. Such effect in some cases is as strong as a judicious characterization of the device is not possible.[12] Although the mesostructured device has demonstrated the best power conversion efficiencies (PCEs)[13] to date, the best choice to stem the hysteresis in perovskite solar cells has foresaid material deposition onto organic transporting layers, as this most probably reduces ions movement/accumulation at the interface, which is the prime suspect of the phenomena.[14,15] Additionally, the use of conformal plastic polymeric transporting layers avoids high-temperature processing and holds important application such as flexible and industrially sustainable photovoltaics.[16,17]

Among the several conductive polymers[18] used as charge transporting layers, the solid polyelectrolyte poly(3,4-ethylenedioxythiophene) polystyrene:sulfonate (PEDOT:PSS) is the most successful anode interfacial material in vision of its simple solution-processability, high conductivity, and transparency.[5,18,19,20,21] The drawbacks of PEDOT:PSS, if compared to inorganic scaffolds, are lower maximum V_{OC} values[16,22,23] and a more tricky control of the perovskite deposition onto a smooth and soft polymeric surface.[24] Furthermore, solution based deposition approaches often encounters dewetting issues, which could affect the realization of highly efficient PHJs.[3,25,26,27,28] Thus, when using a flat surface, enhancing the wettability of the substrate is of paramount importance to encourage heterogeneous material nucleation and decrease the nucleation energy barrier, facilitating the growth of perovskite crystals.[25]

In this frame, a recent work demonstrates how through a modification of the polymer and, in turn, of the surface wettability is possible to increase the heterogeneous nucleation of perovskite.[28] Benefiting from these findings, here we develop a novel nanocomposite based on PEDOT:PSS doped with graphene oxide (GO) and glucose. We demonstrate that the synergistic effect of such dopants modifies the wettability of PEDOT:PSS surface while improving the charge transporting properties of the composite. The effect of the two additives derives from their interesting and complementary properties. Solution processable GO,[29,30,31,32] thanks to different chemical

functionalization,[33] can be exploited to modify the chemical properties of surfaces changing their wettability.[34] [35] [36] Concurrently, glucose molecule has a double effect of favoring the reduction of GO,[37] [38] and of further enhancing the PEDOT:PSS substrate wettability due to the presence of numerous hydroxyl group terminations.[39] The influence of resulting surface tension force on $CH_3NH_3PbI_3$ ($MAPbI_3$) film formation is verified by morphological analyses; the improved morphology of the film growth on the nanocomposite results in photovoltaic (PV) device performances of 12.8%, higher than reference PHJ solar cells based on unmodified PEDOT:PSS (9.4% PCE). Most notably, along with higher current density, we found that the performance enhancement is mainly due to a very high V_{OC}, reaching values over 1.05 V, suggesting minimal recombination losses. Such high V_{OC} values could be explained by X-ray photoelectron spectroscopy (XPS) analysis and cross-section scanning electron microscopy (SEM) imaging, which reveal that a thin insulating caramelized glucose layer forms atop of PEDOT:PSS, leading to a sharp perovskite/PEDOT:PSS interface that could improve the selectivity of the contact.

2 Results and Discussion

2.1 PEDOT:PSS-GO-Glucose Nanocomposite Characterization

Graphene along with its derivatives possesses outstanding mechanical, thermal, and optoelectronic properties, in addition, it could act as protective barriers to gases. These materials can be prepared through various approaches[40] including chemical vapor deposition, mechanical exfoliation, epitaxial growth.[34] Among the various alternatives, we choose solution processable GO as a promising methodology in a prospective of large-scale production,[41] [42] [43] for chemical compatibility with PEDOT:PSS polyelectrolyte and its facile integration into perovskite-based photovoltaic devices.[27] [44] [45]

GO is prepared by a modified Hummers method.[46] [47] [48] The hybrid PEDOT:PSS+GO+glucose nanocomposite, hereafter referred as GGO-PEDOT, and reference PEDOT:PSS+glucose (G-PEDOT) and PEDOT:PSS+GO (GO-PEDOT) composites are prepared by mixing PEDOT:PSS with a dilute dispersion of either GO in water and/or glucose powder (see the Experimental Section for details). The basal plane of a GO sheet is composed of unoxidized graphitic patches and heavily oxidized domains functionalized by hydroxyl and epoxide groups, that guarantees a clear and homogeneous dispersion of GO into PEDOT:PSS polyelectrolyte. The glucose powder is finally added to GO-PEDOT dispersion to form the GGO-PEDOT nanocomposite (**Figure 1**). Nanocomposite films were characterized by SEM, atomic force microscopy (AFM), and X-ray diffraction (XRD) to analyze the dispersion of GO into the polymer matrix; UV–visible spectroscopy and XPS analysis were performed to quantify the effective reduction of GO.

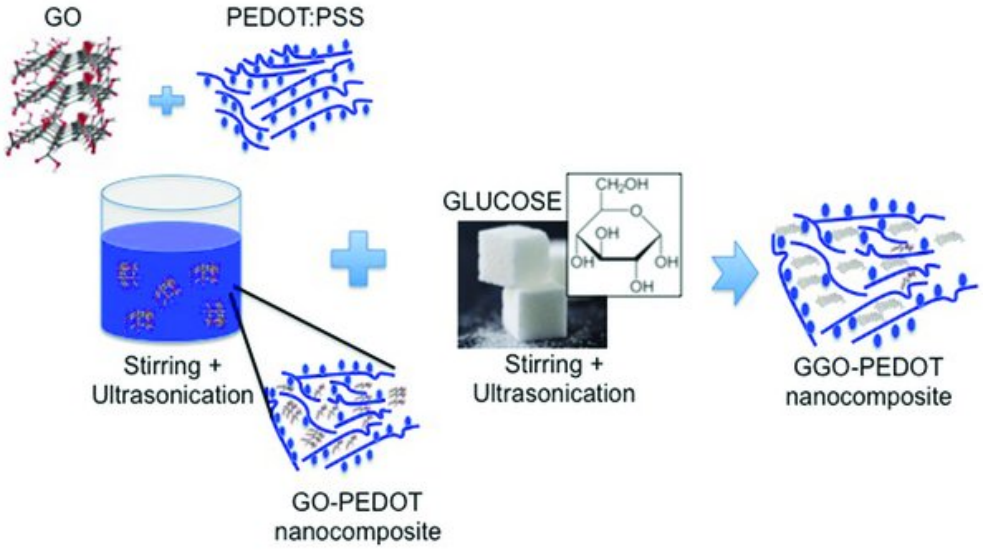

Figure 1 A simplified sketch of the nanocomposite GGO-PEDOT preparation. The hydrophilic edges of GO sheets and the glucose hydroxyl groups favor the dispersion in PEDOT:PSS polyelectrolyte. PEDOT:PSS has a necklace structure in which the hydrophilic PSS segments form blobs decorating the hydrophobic PEDOT chains, allowing a good and homogeneous interaction with hydrophilic GO sheets. **Q2:** [APT to AU] If you have not returned the color cost confirmation form already, please email the completed form to the editorial office when you submit your proof corrections. This will confirm that you are willing to support the cost for color publication of the figures. Details about our color

policies and a link to the form were included with your acceptance email. If you wish for your figures to be presented in greyscale, please email the editorial office to confirm this. [Reply by AU] I will e-mail the black and white figure to the editorial office

Figure 2 reports the XRD patterns of GO,[46,47] compared to that of GO-PEDOT and GGO-PEDOT films drop-casted onto glass substrates, before annealing treatment. Noticeably a sharp peak, (001) reflection centered on 2θ = 11.12°, characteristic of GO, with an interlayer spacing of 0.80 nm, is evidenced.[49] A further broad band is observed for higher angles indicating low-ordered structures due to chemical functionalization of the GO sheets.[50,51] When incorporated in PEDOT:PSS, the main peak disappears indicating that GO sheets do not stack when dispersed in the polymer matrix. The main feature does not roughly change upon addition of glucose, either in GO-PEDOT dispersion or in pure GO in water (Figure S1, Supporting Information), suggesting a good intercalation and, probably, interaction of GO sheets and glucose, which is able to exfoliate and further distance them. This is also confirmed by SEM images of GO-glucose, spin-coated film on indium tin oxide (ITO), showing a homogeneous distribution and a low aggregation of the GO sheets (Figure S2, Supporting Information).

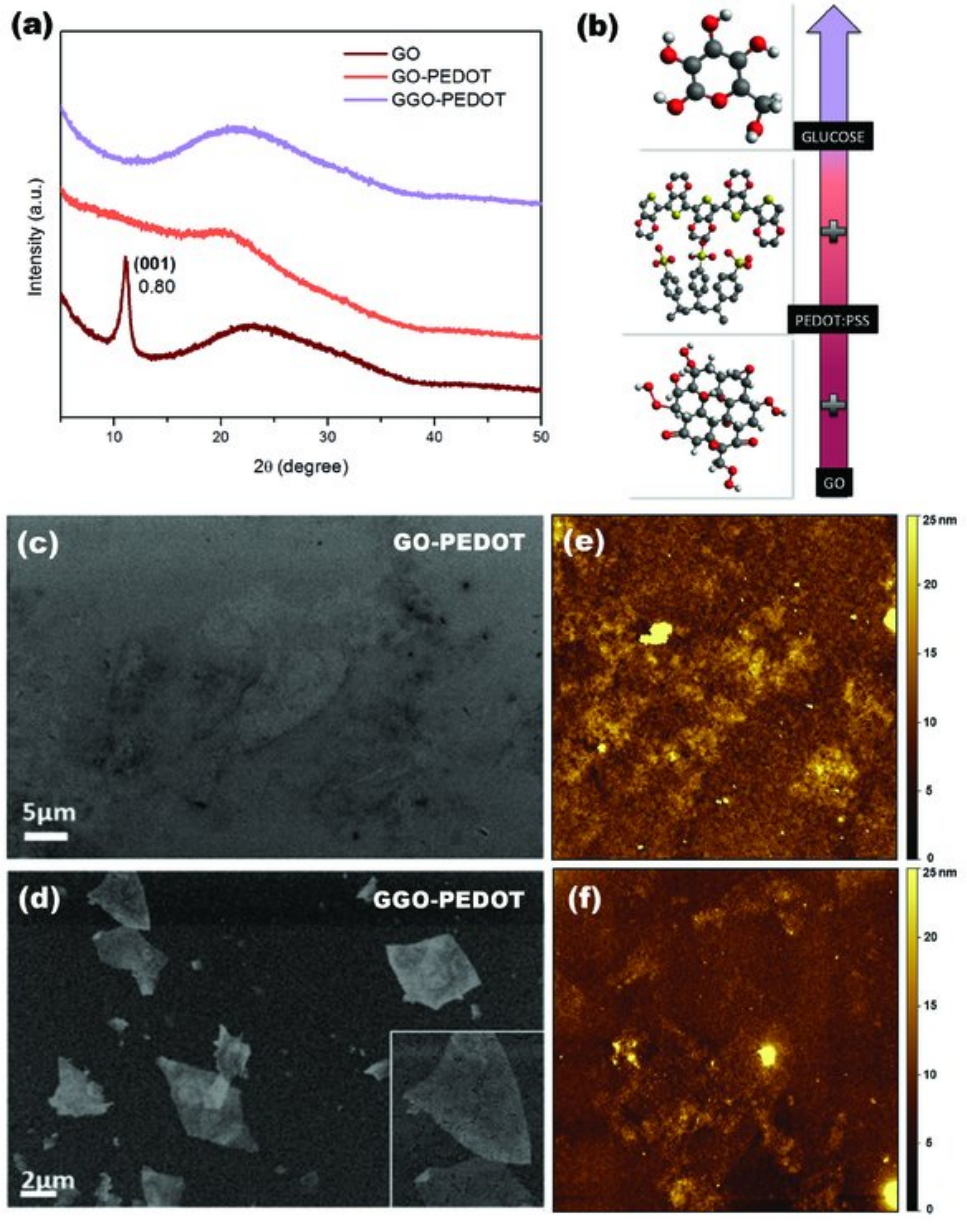

Figure 2 a) Diffraction XRD patterns of GO, GO-PEDOT, and GGO-PEDOT collected in θ–2θ scan mode drop-casted on glass. b) Nanocomposite precursors. SEM images of c) GO-PEDOT and d) GGO-PEDOT nanocomposite films and corresponding AFM micrograph of e) GO-PEDOT (scan area 20 × 20 µm^2, Z-range 25 nm) and f) GGO-PEDOT(scan area 50 × 50 µm^2, Z-range 25 nm).

The morphology of GO-PEDOT and GGO-PEDOT, spin-coated onto ITO, is verified by SEM and AFM inspection (Figure 2). The SEM images of the reference sample of pristine PEDOT:PSS and G-PEDOT:PSS are reported Figure S3 (Supporting Information) for comparison. GO-PEDOT forms a continuous film, albeit with some aggregates, possibly due to stacked GO sheets. Whereas the GGO-PEDOT film results homogeneous and the GO

sheets are evenly dispersed in the polymer matrix. It is even possible, in this case, to observe the single GO sheet. The steric bonding of glucose to the carbon of GO could favor the dispersion of GO through a lower aggregation of the sheets, facilitating the formation of a homogeneous GGO-PEDOT film. These results first confirm a good blending of GO in the PEDOT:PSS and a π–π* electron donor–accepter interaction between GO and PEDOT:PSS.[52]

According to literature, the addition of glucose in the GO suspension and thermal annealing in nitrogen atmosphere could facilitate the GO reduction process.[37,38] In order to verify this hypothesis, we measure UV–visible absorption (Figure S4, Supporting Information) as a first direct instrument to see changes in GO before and after reduction.[34] The inset in Figure S4c (Supporting Information) shows a photograph of the GO+glucose film variation from light brown to black color after annealing at 140 °C for 1 h, ascribable to the absorption of K- and B-band of aromatic compounds indicating a reduction.[53,54] Upon glucose addition and annealing, the shoulder at 300 nm (n → π* transitions of C═O bonds) in the absorption spectra of GO disappears and the peak at ≈230 nm (π → π* transitions of aromatic C─C bonds) shifted to 265 nm, suggesting the restoration of the electronic conjugation within the graphene sheets.[51,54] No differences could be observed in the absorption spectra of pure Glucose and GO separately before and after annealing at 140 °C (Figure S4a,b, Supporting Information), suggesting that the shift in the GO spectra could be ascribed to reduction induced by glucose. Such an optical modification in the GGO-PEDOT:PSS cannot be observed because the absorption spectrum of bare PEDOT:PSS superimposes to the GO and reduced GO characteristic peaks[52,55] (Figure S4d, Supporting Information). No differences could be observed in the absorption spectra of PEDOT:PSS adding glucose and GO, after annealing at 140 °C (Figure S5, Supporting Information).

In order to follow the reduction process and to study the properties of hybrid GGO-PEDOT films, all of the stages for the preparation of the nanocomposites are monitored by XPS measurements. In particular, we analyzed carbon (C) and oxygen (O) species on four stages: (i) pristine PEDOT:PSS, (ii) GO-PEDOT, (iii) GGO-PEDOT, and (iv) annealed GGO-PEDOT films (see the Supporting Information for more details).

The chemical modification of the system is quantified by evaluating the ratio between carbon and oxygen atoms (C/O). **Figure 3**a reports the C/O ratio measured on pristine PEDOT:PSS film at increasing the GO concentration in solution in the range between 0 and 0.25% (wt/vol) (Table S1, Supporting Information). In the case of pure polymer film, the measured C/O ratio amounts to 27 ± 3 indicates the presence of the phase segregation of the PEDOT:PSS film, resulting in a predominance of PSS in the surface region[56] with the corresponding decreasing of the oxygen content at the PEDOT:PSS surface (see Figure S6 and Table S1 in the Supporting Information). Adding GO to the film (C/O (GO) = 2.7 ± 0.3), the total amount of oxygen increases corresponding to a decreasing of the measured C/O ratio: C/O (GO) < C/O (measured) < C/O (PEDOT:PSS). A similar trend, albeit with higher C/O ratio, is observed after the annealing due to a partial reduction of GO in Figure 3a and Table S1 (Supporting Information). The slightly scattered trend could be ascribed to little variations of GO concentration on the PEDOT:PSS surface caused by the inhomogeneous distribution of GO sheets in the PEDOT:PSS matrix in absence of glucose, as evidenced from morphological characterization (Figure 2).

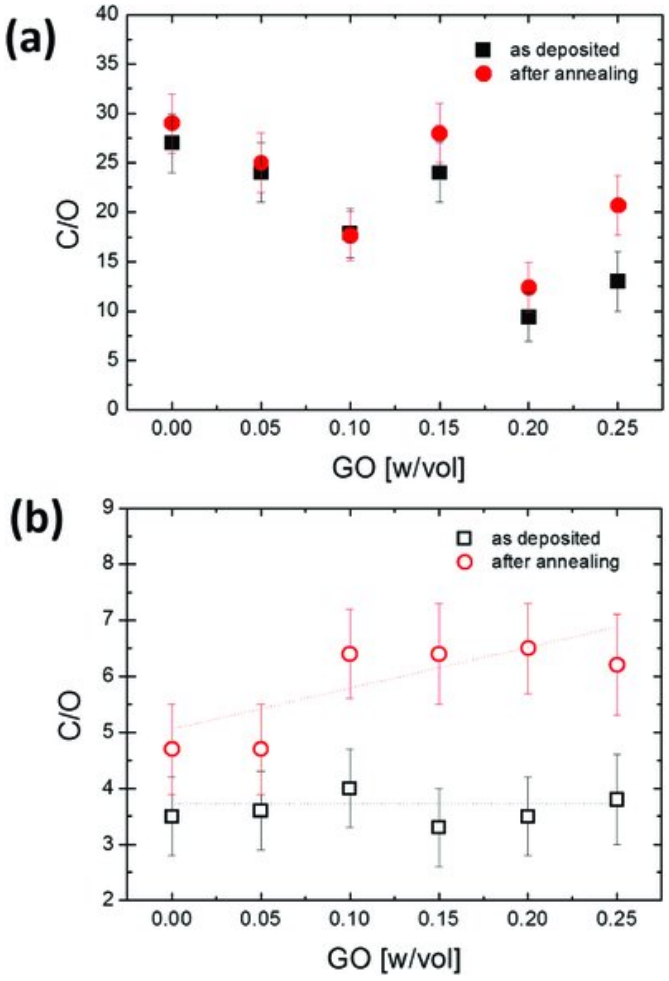

Figure 3 C/O ratio measured at different GO concentrations on a) PEDOT:PSS and b) G-PEDOT films. Measurements are performed before and after the thermal annealing of the samples.

The same approach is used to study the film with glucose, as shown in Figure 3b in which we used the same color code to compare the measured values before and after the annealing. The presence of glucose changes the C/O ratio from 27 ± 3 to 13 ± 3 before the addition of GO. Taking into account the stoichiometric value of pure glucose (C/O = 1)[57] and the surface-sensitivity of the XPS technique (ca 5 nm thick) we evinced that glucose does not disperse uniformly in the vertical section of the film and, closer to the surface, the G-PEDOT is mainly composed by glucose (ca 90%). The addition of GO to the G-PEDOT composite film does not significantly change the measured C/O ratio. This is an expected experimental trend because the C/O ratio of GO is 2.7 ± 0.3. Upon the annealing at 140 °C, the C/O ratio increases to 4.8 ± 0.8 without GO, indicating a partial caramelization of glucose,[58] and roughly increases linearly with GO concentration (dash line) ascribable to the reduction of GO. (Figure 3b and Table S2 (Supporting Information)).

The thermal stability of pristine PEDOT:PSS and doped PEDOT:PSS was investigated by thermogravimetric analysis (TGA) and differential scanning calorimetry (DSC) analysis (Table S3, Supporting Information). The TGA curves of the films show two principal weight loss steps (Figure S7, Supporting Information). The first one, from 20 to about 160 °C, combined with the broad endothermic peak observed with the DSC analysis, indicates that the film releases water during the heating process.[59] The characteristic dehydration energy calculated for all the films is in the range of the energy of moderate hydrogen bonds (10–60 kJ mol^{-1}). The characteristic dehydration energy for the PEDOT:PSS decreases from 39 to 33 kJ mol^{-1} adding GO and to 22 kJ mol^{-1} adding glucose, showing a different interaction with water molecules influenced by the presence of doping elements in the PEDOT:PSS. In the film with both GO and glucose, the characteristic dehydration energy decreases down to 12 kJ mol^{-1} suggesting that water molecules are weakly bound and can evaporate more easily than other systems, influencing film formation. The second weight loss, from 250 to about 500 °C, is due to oxidizing decomposition of the skeletal PEDOT and/or PSS backbone chain structure.[60] In particular, at ≈250 °C and over 350 °C, the PSS sulfonate group fragmentation and the carbon oxidation occur, respectively.[61] All the films are thermally stable below 250 °C, consequently no degradation occurs during annealing treatment (140 °C).

The contribution of glucose and GO on the electrical properties of the film after the annealing was studied performing DC electrical measurements with four-points probe. The measured sheet resistance values are reported in **Table 1**. The sheet resistance measured on pure PEDOT:PSS film amounts 50 MΩ □ $^{-1}$ and agrees with literature.[62] Adding only glucose, the G-PEDOT film became an insulator (resistance > GΩ □$^{-1}$), in agreement with the XPS analysis indicating the presence of glucose mainly on the film surface. Conversely, the resistance decreases by adding of GO. In general, by adding glucose and GO or GO only the electrical behavior is quasi-ohmic as in the case of pure PEDOT:PSS while the charge-injection decreases.

Table 1 Sheet resistances of film after annealing

	PEDOT:PSS	GO-PEDOT	G-PEDOT	GGO-PEDOT
Sheet resistance	50 ± 5 [MΩ □$^{-1}$]	180 ± 20 [kΩ □$^{-1}$]	10 ± 2 [GΩ □$^{-1}$]	1.9 ± 0.2 [MΩ □$^{-1}$]

2.2 GGO-PEDOT/Perovskite Heterojunction

The wettability of the diverse PEDOT:PSS based nanocomposite on ITO and of perovskite precursors on the different nanocomposites was evaluated by contact angle measurements (**Figure 4**a,b). The addition of both GO and glucose into PEDOT:PSS reduces the contact angle of PEDOT:PSS based solutions on ITO substrate from 93.6° ± 3.1° to 77.6° ± 3.7° (Figure 4a), ensuring a good coverage and electrical contact at the anode. Importantly, the contact angles of perovskite precursor solutions on the different substrates decrease upon the addition of GO and glucose reaching the minimum value of 5.1° ± 1.1° on GGO-PEDOT:PSS (Figure 4b). These results demonstrate that GGO-PEDOT shows a superior wettability and compatibility with perovskite precursor solution, enabling the formation of high coverage uniform perovskite films that was relevant for fabrication of devices, as can be observed from SEM images in Figure 4c. It can be readily observed that the perovskite film grown on GGO-PEDOT shows more compact and closer grains, leading to less intergrain spaces and cracks if compared to perovskite grown on pristine PEDOT:PSS. AFM images in Figure S8 (Supporting Information) show how the wettability also impacts on the film roughness, which decreases from R_q ≈ 10 nm for PEDOT:PSS down to R_q ≈ 8 nm for GGO-PEDOT. The crystalline structure of the perovskite films, instead, remains unvaried (XRD spectra in Figure S9, Supporting Information).

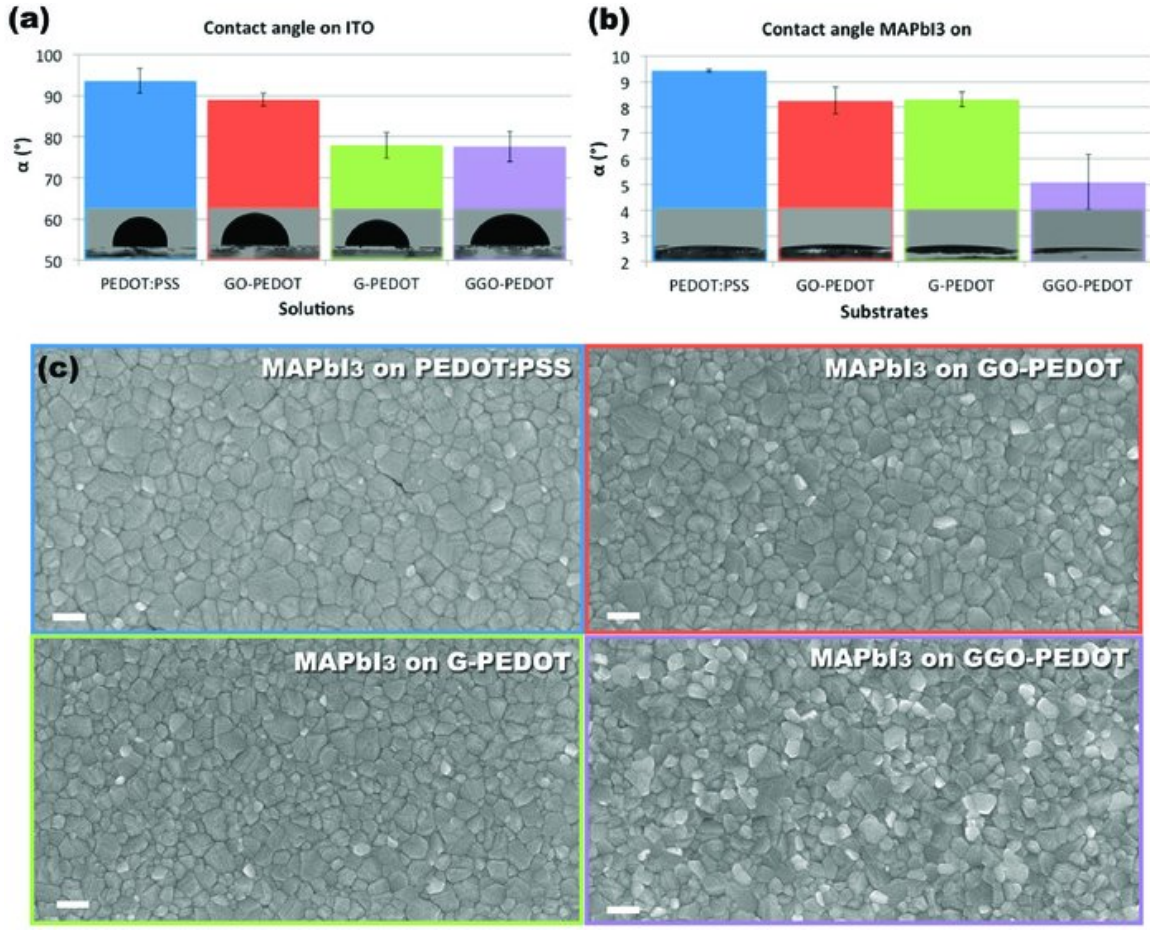

Figure 4 a) Contact angle of pristine PEDOT:PSS, GO-PEDOT, G-PEDOT, and GGO-PEDOT on ITO and b) Contact angle of perovskite precursor drops on PEDOT:PSS, GO-PEDOT, G-PEDOT, and GGO-PEDOT nanocomposite substrates. c) SEM morphology for perovskite material deposited on the different nanocomposite substrates.

2.3 Hybrid Perovskite Solar Cells with Nanocomposite Hole Transporting Layers

The GGO-PEDOT:PSS nanocomposite film was implemented in a perovskite based solar cells to examine the doping influence on the performance of the hybrid device. For comparison, devices with GO-PEDOT nanocomposite, G-PEDOT, and bare PEDOT:PSS were also made.

In each device realized, the perovskite layer, which acts as a light absorber, was deposited by spin-coating on top of the PEDOT:PSS based layer. The perovskite precursors were prepared as described in previous work,[63] and $MAPbI_3$ smooth and homogeneous active layer was obtained by a modified nonsolvent dripping method.[5]

In **Figure 5**, we report the *J–V* characteristic and performance of the best device based on the GGO-PEDOT:PSS, compared with pristine PEDOT:PSS, GO-PEDOT, and G-PEDOT. Statistics on the FF, V_{OC}, J_{SC}, PCE for all the devices tested and the incident photon to current efficiency (IPCE) are reported in Figures S10 and S11 (Supporting Information).

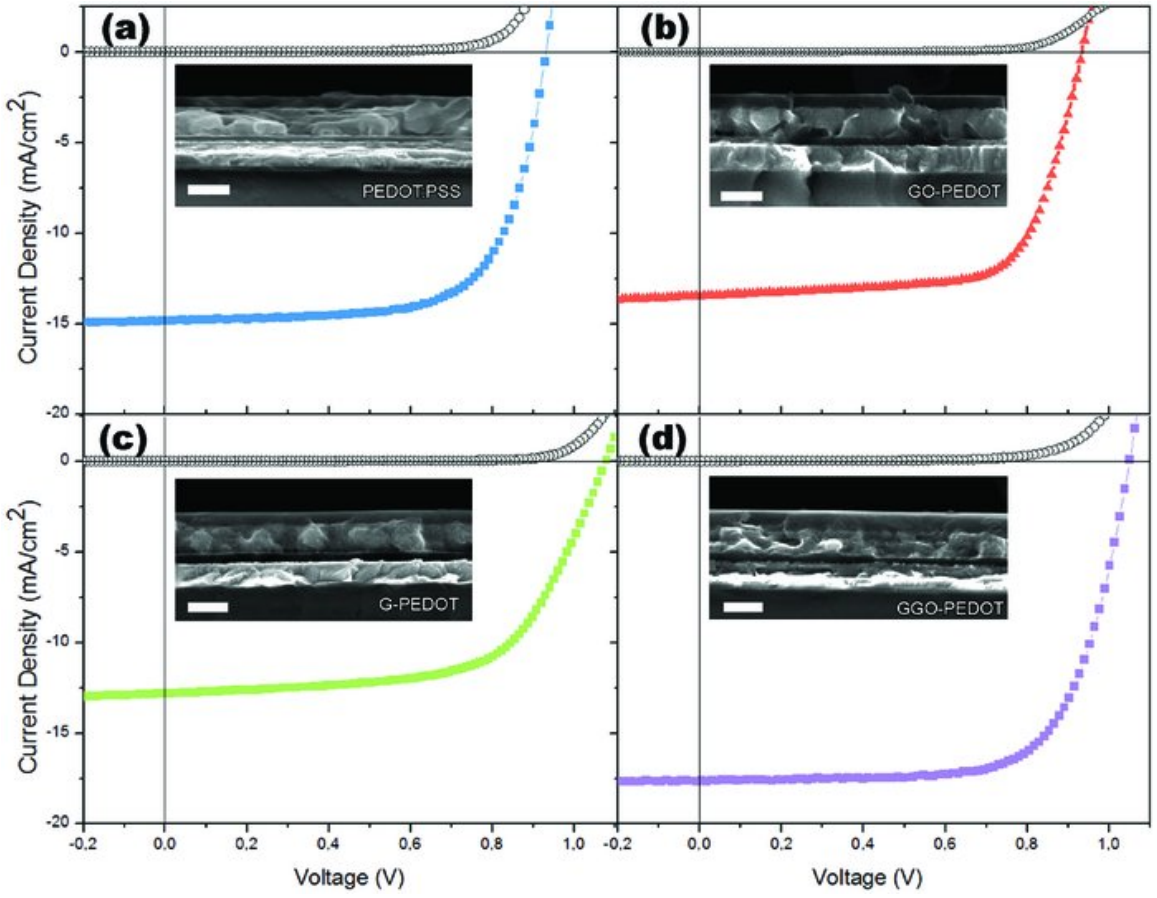

Figure 5 Current density versus applied bias (*J–V*) characteristics under AM 1.5G (100 mW cm^{-2}) simulated solar illumination (filled symbols) and in the dark (open symbols) for a) PEDOT:PSS, b) GO-PEDOT, c) G-PEDOT, and d) GGO-PEDOT based best devices; SEM cross-section of the devices in the inset.

The perovskite device made on GGO-PEDOT results in the best performing devices (see **Table 2** and Figure 5), reaching a maximum PCE of 12.8%, with no hysteresis (see Figure S12 in the Supporting Information). Along with higher current density, we found that the improvement is mainly due to a very high V_{OC}, suggesting minimal recombination losses and very efficient electron and hole extraction at the electrodes. As can be seen from Figure S12 (Supporting Information), V_{OC} maximum reaches values over 1.05 V that are among the highest ever reported for PHJ inverted architecture with PEDOT:PSS hole transporting layer,[22] which usually shows a slight V_{OC} drop if compared to the conventional n-i-p PHJ solar cells.[16] Usually, this problem is overcome by the insertion of an electron blocking polymer interlayer between PEDOT:PSS and perovskite,[64,65] but these polymers are usually hydrophobic, thus making the deposition of perovskite by solution processing impossible. Conversely, our approach

offers the advantage of enhancing the solar cell V_{OC}, while improving the wettability of PEDOT:PSS for perovskite precursors. The high V_{OC} could potentially indicate that the perovskite film grown on GGO-PEDOT is of a high quality, with low surface/sub-bandgap states, and considering the very thin perovskite layer (≈160 nm), the device performances are remarkable.[64] As high performing semitransparent solar cells, bearing thin active perovskite layer, instead of thicker opaque devices foresees great technological impact aiming the implementation of photovoltaic devices into building integrated elements, such as windows or portable electronic devices.[66,67,68,69,70]

Table 2 Best performance and average values of the devices based on GGO-PEDOT compared with that of PEDOT:PSS, GO-PEDOT, and G-PEDOT

Layer		J_{SC} [mA cm^{-2}]	V_{OC} [V]	FF	PCE [%]
GGO-PEDOT	rev	17.6	1.05	0.69	12.8
	average	14.3 ± 2.3	1.00 ± 0.07	0.66 ± 0.06	9.6 ± 1.9
PEDOT:PSS	rev	14.9	0.93	0.68	9.4
	average	12.0 ± 2.1	0.9 ± 0.1	0.72 ± 0.05	7.8 ± 1.3
GO-PEDOT	rev	13.5	0.93	0.69	8.7
	average	10.8 ± 1.5	0.89 ± 0.05	0.71 ± 0.02	6.8 ± 1.1
G-PEDOT	rev	12.8	1.08	0.63	8.7
	average	12.1 ± 2.7	1.01 ± 0.07	0.63 ± 0.03	7.5 ± 1.0

The V_{OC} amelioration, albeit accompanied to a reduction in the J_{SC} and FF values, is also observed when only glucose is added to PEDOT:PSS. In this case (G-PEDOT), we obtain V_{OC} values up to 1.08 V, we attribute such a high value to the formation of a thin insulating caramelized glucose layer atop of PEDOT:PSS. This thin insulting layer could either act as an electron blocking, as it happens for insulating Al_2O_3,[71] and/or could modify the PEDOT:PSS work-function.[72] Moreover, the thin interfacial layer of glucose could, in analogy to what recently reported for Lewis bases,[73] passivate the halide vacancies at the grain boundaries of perovskite polycrystals which act as charge trapping states. Thus the observed higher V_{OC} for the glucose based nanocomposites can be ascribed to the trap density reduction at the perovskite/PEDOT:PSS.

We calculate the series resistance for the pristine PEDOT:PSS (R_s = 11.4 Ω cm^2), GGO-PEDOT (R_s = 13.7 Ω cm^2), G-PEDOT (R_s = 18.4 Ω cm^2), and GO-PEDOT (R_s = 56.0 Ω cm^2) best performing devices and we find that upon addition of either GO or glucose in PEDOT:PSS, the series resistance increases. Whereas in the complete GGO-PEDOT nanocomposite, the R_s recovers approaching values as low as pristine PEDOT:PSS. Considering this, the reduction in the J_{SC} and FF values in G-PEDOT can be due to the formation of the thin insulating caramelized glucose layer atop of PEDOT:PSS, partially blocking the charge collection at the ITO electrode.[74] However, in the complete GGO-PEDOT nanocomposite, considering the higher J_{SC} and FF and lower R_s values, this effect is less pronounced and likely mitigated by the better morphology of the perovskite active layer.

From cross-section SEM inspection (inset Figure 5), it can be noted that the perovskite interface with GGO-PEDOT and, more evidently, G-PEDOT films is sharper than that with GO-PEDOT and pristine PEDOT:PSS, where some interfusion seems to occur. Such a net interface could improve the hole-selectivity of the contact and contribute to the V_{OC} enhancement.

Overall, in the ternary nanocomposite GGO-PEDOT, the cooperative effect of reduced GO and glucose, improves the conduction properties of PEDOT:PSS and modifies the sensible interface, leading to superior performance if compared to the pristine PEDOT:PSS hole transporting layer. The GO-PEDOT composite leads to a slight decrease in photocurrent and fill factor.

3 Conclusion

In conclusion, we demonstrate here the synergic positive effect of GO and glucose in affecting the PEDOT:PSS surface and electrical properties. The combined effort of glucose and GO increases the performance of the device

because the insulating layer of glucose changes the surface wettability, improving the homogeneity of the upper PEDOT:PSS layer, while the presence of reduced GO sheets restores and improves the electrical conductibility of the film.

To our purpose, the enhanced substrate wettability guarantees a good interaction of the perovskite precursors with the doped GGO-PEDOT underlayer. The influence of resulting surface tension force on $MAPbI_3$ film formation is verified by morphological analyses. The improved film morphology from one side, and the formation of a net interface with the hole transporting layer results in improved photovoltaic device performances. The hybrid GGO-PEDOT nanocomposite in particular shows outstanding V_{OC}, evidencing minimal recombination losses, high hole-selectivity, and reduced trap density at the PEDOT:PSS along with optimized $MAPbI_3$ coverage.

Our study offers a promising approach to guide the formation of uniform and high coverage perovskite film on flat polymeric substrate, allowing also intelligent interface engineering for an overall improving of the device performance.

A further interesting advantage of our approach is that, if compared to other GO reduction processes requiring harsh temperature (up to 800 °C)[75] or highly toxic reducing agent (such as hydrazine, hydroquinone, sodium borohydride),[34] it represents a mild-temperature and a green alternative strategy, fully compatible with large-scale production of nanocomposite films.

4 Experimental Section

Synthesis of GO: GO was prepared using a modified Hummers method[46,47] yielding GO flakes with a maximum lateral size of 100 µm. The prepared GO solution in water (2 mg mL^{-1}) was stable for more than one year as confirmed by UV–vis absorption measurements. AFM was used to monitor the abundance of single layers (>95%) by spin-coating the solution on ultraflat silicon oxide surface.

PEDOT:PSS-GO-Glucose Nanocomposite Preparation and In Situ GO Reduction: PEDOT:PSS aqueous solution (Clevios PVP AI4083) was purchased from Heraeus with a PEDOT:PSS concentration of 1.3% by weight and the weight ratio of PSS to PEDOT was 6. α-D-glucose anhydrous 96% (glucose) was purchased from Sigma-Aldrich. The dispersion of GO into PEDOT:PSS, commercially available as Clevios PVP AI4083, was obtained by the solvent swelling method, previously developed.[76,77] GO was added into PEDOT:PSS with a concentration of 0.05 wt%/vol%. Concentrations of 0.10%, 0.15 %, 0.20%, and 0.25% (wt/vol) were explored for XPS analysis. **Q3:** [APT to AU] The expression '% wt/V' has been changed to 'wt%/vol%' throughout text. Please check for correctness. [Reply by AU] no, it is better to write: % (wt/vol) After 90 min of stirring and 15 min of sonication at room-temperature (RT), 1% (wt/vol) of glucose was added to a GO-PEDOT:PSS dispersion, stirring and sonicating for 15 min, respectively. **Q4:** [APT to AU] The symbols ' and ' have been changed to min and s, respectively, throughout the text. Please check for correctness. [Reply by AU] ok The film of GGO-PEDOT was obtained by spin coating of solution on an ITO substrate at 3000 rpm for 60 s in air at RT and annealed at 140 °C for 1 h in glovebox in a nitrogen atmosphere. Dispersions and films of GO-PEDOT and of G-PEDOT were prepared by the same procedure to understand the influence of all the doping separately.

The GO ex situ reduction was performed adding 1% (wt/vol) of glucose in the GO/water dispersion (0.05% wt/vol) by stirring and sonicating for 15 min, respectively. The dispersion was deposited at RT in air on different substrates and treated at 140 °C for 1 h in glovebox in a nitrogen atmosphere.

XRD: The XRD spectra of the prepared films were recorded with a PANalytical X'Pert-PRO Materials Research Diffractometer using graphite-monochromated CuKα radiation (λ = 1.5405 Å).

Morphological Characterization: Scanning electron microscope images of the samples were recorded using Carl Zeiss Auriga40 Crossbeam instrument, in high vacuum and high-resolution acquisition mode, equipped with Gemini column and an integrated high efficiency in-lens detector. The applied acceleration voltage was 2 or 5 kV. AFM imaging was carried out in air using a Park Scanning Probe Microscope (PSIA) operating in a noncontact mode to reduce tip induced surface degradation and sample damage. The image acquisition was performed in air at room temperature.

UV–Vis Absorption: The GO/glucose dispersion was drop casted on a quartz substrate and analyzed by UV–

visible spectrophotometer (Varian Cary 500) before and after thermal annealing to evaluate the efficiency of the GO reduction reaction through glucose. The Ultraviolet–visible absorption spectra were recorded on spectrophotometer in the 200–800 nm wavelength range at room temperature.

XPS: The XPS spectra were recorded with a Phoibos 100 hemispherical energy analyzer (Specs) using Mg Kα radiation ($\hbar\omega$ = 1253.6 eV). The X-ray power was 250 W. The spectra were recorded in the constant analyzer energy mode with analyzer pass energies of 40 eV for the survey spectra and 20 eV for the high resolution ones. Charging effects were corrected by energy calibration on C 1s level relative to 284.5 eV. The base pressure in the analysis chamber during analysis was 3×10^{-10} mbar.

Contact Angle Measurement: The wettability of the different substrates was evaluated by contact angle measurements with a First Ten Angstroms FTA1000 Quick Start instrument.

TGA-DSC Characterization: Thermogravimetric analyses were carried out on a TGA/DSC 1 manufactured by Mettler Toledo, under a nitrogen atmosphere created by fluxing 50 mL min^{-1} of N2 from 20 to 600 °C at the heating rate of 10 °C min^{-1}. About 5 mg of sample was put into alumina pan for the test, after air-drying for 96 h samples were drop casted on cleaned silicone sheet. The results obtained from TGA in the range of 20–160 °C were combined with the analysis by a differential scanning calorimeter (DSC Mettler Toledo 622) to understand the reaction that occurred in all the systems. About 5 mg of dried samples for 96 h on silicone sheet were put into aluminum flat disks and heated from 20 up to 160 °C at 10 °C min^{-1} under nitrogen atmosphere flow at 80 mL min^{-1}. After free cooling to room temperature, a second heating scan was performed. Combining DSC and TGA results together provide more refined information about the water loss and the energy associated to the loss of itself, calculating the characteristic energy for dehydration (Equation (1)) Q5: [APT to AU] Please check all equations have been correctly typeset. [Reply by AU] ok

$$E = M\,(\Delta Q/\Delta W) \tag{1}$$

where M was the water molecular weight (18 g mol^{-1}), ΔQ was the amount of heat absorbed during the dehydration, estimated from DSC, and ΔW was the weight loss of water estimated from TGA, both between 20 and 160 °C.

Four-Points Probe Measurements: The sheet resistance of the film was measured with a four-point probe system in Van der Pauw geometry (probed area of 10 × 10 mm^2, H50 Hall Effect Controller, MMR Technologies), while the two-probe measurements by home-made system (Keithley 6517A/Keithley 6514).

Device Fabrication and Testing: Glass with precoated ITO thin film was used as substrate. It was cleaned with acetone, water, and isopropanol in an ultrasonic bath for 10 min each. Finally, it was immersed into a TL1 washing solution ($H_2O_2/NH_3/H_2O$ 5:1:1, v/v) and heated at 80 °C for 10 min to remove organic contamination, then rinsed ten times in water. Either pristine PEDOT:PSS, GO-PEDOT, G-PEDOT, or GGO-PEDOT solutions were then spin-coated on the ITO substrate at 3000 rpm for 60 s in air atmosphere. The coated film was first dried at about 70 °C for 5 min and then annealed at 140 °C for 1 h in N_2 atmosphere. Briefly, methylamine (CH_3NH_2) solution, 33 wt% in absolute ethanol, was reacted with hydroiodic acid (HI), 57 wt% in water, with excess methylamine under a nitrogen atmosphere in ethanol at room temperature. Typical quantities were 24 mL of methylamine, 10 mL of HI, and 100 mL of ethanol. Crystallization of methylammonium iodide (MAI) was achieved using a rotary evaporator; a white-colored powder was formed, indicating successful crystallization. MAI and lead (II)iodide (PbI_2) (Aldrich) were stirred in a mixture of dimethyl sulfoxide:γ-butyrolactone (1:2, v/v) at 60 °C for about 30 min. In details, the 40% $MAPbI_3$ perovskite precursor solution was spin-coated onto PEDOT:PSS based/ITO substrate by a consecutive two-step spin-coating process at 1000 and 4000 rpm for 20 and 60 s, respectively, and the dichloromethane in final spin-stage was dripped onto the substrate during spin-coating. Then the coated substrate was annealed on a hot plate at 100 °C for 10 min. A chlorobenzene solution of phenyl-C61-butyric acid methyl ester (25 mg mL^{-1}) layer was deposited by spin-coating at 1000 rpm for 60 s. Finally, the device was completed with evaporation in a high vacuum of Al contact electrodes after evaporation of LiF (≈0.5 nm) layer through shadow mask.[39] The active area of Al electrodes in the fabricated device was 0.04 cm^2. Each device was characterized under air mass 1.5 global (AM 1.5G) solar simulator with an irradiation intensity of 100 mW cm^{-2}. Current–voltage characteristics of the PV devices were studied using a Keithley 2400 Source Measure Unit and a solar simulator Spectra Physics Oriel 150 W with AM 1.5G filter set. The measurement was made setting a range of voltage from 1.1 to −0.5 V in reverse mode.

The IPCE was measured by the DC method using a computer-controlled xenon arc lamp (Newport, 140 W, 67005) coupled with a monochromator (Newport Cornerstore 260 Oriel 74125). The light intensity was measured by a calibrated silicon UV-photodetector (Oriel 71675) and the short circuit currents of the solar cells were measured by using a dual channel optical power/energy meter (Newport 2936-C).

+No. Supporting Information

Supporting Information is available from the Wiley Online Library or from the author.

Acknowledgements

The authors acknowledge Caripuglia for funding the project “Nanocompositi polimerici innovativi a base di grafene da utilizzare come controelettrodi di celle solari solide mesostrutturate di nuova concezione” 2014. A.R. gratefully acknowledges SIR project “Two-Dimensional Colloidal Metal Dichalcogenides based Energy-Conversion Photovoltaics” (2D ECO), Bando SIR (Scientific Independence of young Researchers) 2014 MIUR Decreto Direttoriale 23 gennaio 2014 no. 197 (project number RBSI14FYVD, CUP: B82I15000950008) for funding. A. Liscio acknowledges Graphene Flagship (Grant Agreement No. 604391). S.C. and A. Listorti acknowledge Regione Puglia and ARTI for funding FIR – future in research projects “PeroFlex” project no. LSBC6N4 and “HyLight” project no. GOWMB21.The authors acknowledge Sonia Carallo and Derek Jones for technical support.

+ 1 W. S. Yang, J. H. Noh, N. J. Jeon, Y. C. Kim, S. Ryu, J. Seo, S. I. Seok, *Science* **2015**, *348*, 1234.

+ 2 A. Listorti, E. J. Juarez-Perez, C. Frontera, V. Roiati, L. Garcia-Andrade, S. Colella, A. Rizzo, P. Ortiz, I. Mora-Sero, *J. Phys. Chem. Lett.* **2015**, *6*, 1628.

+ 3 M. Liu, M. B. Johnston, H. J. Snaith, *Nature* **2013**, *501*, 395.

+ 4 S. Masi, S. Colella, A. Listorti, V. Roiati, A. Liscio, V. Palermo, A. Rizzo, G. Gigli, *Sci. Rep.* **2015**, *5*, 7725.

+ 5 J. Seo, S. Park, Y. C. Kim, N. J. Jeon, J. H. Noh, S. C. Yoon, S. I. Seok, *Energy Environ. Sci.* **2014**, *7*, 2642.

+ 6 B. Cai, Y. Xing, Z. Yang, W.-H. Zhang, J. Qiu, *Energy Environ. Sci.* **2013**, *6*, 1480.

+ 7 J. H. Heo, S. H. Im, J. H. Noh, T. N. Mandal, C.-S. Lim, J. A. Chang, Y. H. Lee, H.-J. Kim, A. Sarkar, M. K. Nazeeruddin, M. Grätzel, S. I. Seok, *Nat. Photonics* **2013**, *7*, 486. **Q6:** [APT to AU] Please check the presentation of author names 'S. H. Im' and 'S. II Seok' in ref. 7 for correctness. [Reply by AU] corrected

+ 8 M. A. Green, T. Bein, *Nat. Mater.* **2015**, *14*, 559.

+ 9 M. Grätzel, *Nat. Mater.* **2014**, *13*, 838.

+ 10 N.-G. Park, *Mater. Today* **2015**, *18*, 65.

+ 11 T. Leijtens, E. T. Hoke, G. Grancini, D. J. Slotcavage, G. E. Eperon, J. M. Ball, M. De Bastiani, A. R. Bowring, N. Martino, K. Wojciechowski, *Adv. Energy Mater.* **2015**, *5*, 1500962. **Q7:** [APT to AU][Please provide page number in refs. (11, 20, 24, 29, 36, 68, 77), if now available.] Reply

+ 12 B. C. O'Regan, P. R. F. Barnes, X. Li, C. Law, E. Palomares, J. M. Marin-Beloqui, *J. Am. Chem. Soc.* **2015**, *137*, 5087.

+ 13 M. A. Green, K. Emery, Y. Hishikawa, W. Warta, E. D. Dunlop, *Prog. Photovoltaics* **2015**, *23*, 1

+ 14 D. Bryant, S. Wheeler, B. C. O'Regan, T. Watson, P. R. F. Barnes, D. Worsley, J. Durrant, *J. Phys. Chem. Lett.* **2015**, *6*, 3190.

+ 15 H.-S. Kim, I.-H. Jang, N. Ahn, M. Choi, A. Guerrero, J. Bisquert, N.-G. Park, *J. Phys. Chem. Lett.* **2015**, *6*, 4633.

+ 16 L. Meng, J. You, T.-F. Guo, Y. Yang, *Acc. Chem. Res.* **2015**, *49*, 155. **Q8:** [APT to AU] Please provide volume and page numbers in refs. (16, 23, 76), if now available. [Reply by AU] corrected

+ 17 S. Masi, A. Rizzo, F. Aiello, F. Balzano, G. Uccello-Barretta, A. Listorti, G. Gigli, S. Colella, *Nanoscale* **2015**, *7*, 18956.

+ 18 J. Y. Jeng, Y. F. Chiang, M. H. Lee, S. R. Peng, T. F. Guo, P. Chen, T. C. Wen, *Adv. Mater.* **2013**, *25*, 3727.

+ 19 J. You, Z. Hong, Y. M. Yang, Q. Chen, M. Cai, T.-B. Song, C.-C. Chen, S. Lu, Y. Liu, H. Zhou, *ACS Nano* **2014**, *8*, 1674.

+ 20 P. Docampo, J. M. Ball, M. Darwich, G. E. Eperon, H. J. Snaith, *Nat. Commun.* **2013**, *4*, 2761.

+ 21 S. Sun, T. Salim, N. Mathews, M. Duchamp, C. Boothroyd, G. Xing, T. C. Sum, Y. M. Lam, *Energy Environ. Sci.* **2014**, *7*, 399.

22 C.-H. Chiang, Z.-L. Tseng, C.-G. Wu, *J. Mater. Chem. A* **2014**, *2*, 15897.

23 Y. Hou, W. Chen, D. Baran, T. Stubhan, N. A. Luechinger, B. Hartmeier, M. Richter, J. Min, S. Chen, C. O. R. Quiroz, *Adv. Mater.* **2016**, *28*, 5112.

24 H. Choi, C.-K. Mai, H.-B. Kim, J. Jeong, S. Song, G. C. Bazan, J. Y. Kim, A. J. Heeger, *Nat. Commun.* **2015**, *6*, 7348.

25 G. E. Eperon, V. M. Burlakov, P. Docampo, A. Goriely, H. J. Snaith, *Adv. Funct. Mater.* **2014**, *24*, 151.

26 T. Salim, S. Sun, Y. Abe, A. Krishna, A. C. Grimsdale, Y. M. Lam, *J. Mater. Chem. A* **2015**, *3*, 8943.

27 Z. Wu, S. Bai, J. Xiang, Z. Yuan, Y. Yang, W. Cui, X. Gao, Z. Liu, Y. Jin, B. Sun, *Nanoscale* **2014**, *6*, 10505.

28 J. You, Y. M. Yang, Z. Hong, T.-B. Song, L. Meng, Y. Liu, C. Jiang, H. Zhou, W.-H. Chang, G. Li, *Appl. Phys. Lett.* **2014**, *105*, 183902.

29 C. Bi, Q. Wang, Y. Shao, Y. Yuan, Z. Xiao, J. Huang, *Nat. Commun.* **2015**, *6*, 7747.

30 T. Liu, D. Kim, H. Han, A. R. bin Mohd Yusoff, J. Jang, *Nanoscale* **2015**, *7*, 10708.

31 A. Fallahi, M. Alahbakhshi, E. Mohajerani, F. A. Taromi, A. R. Mohebbi, M. Shahinpoor, *J. Phys. Chem. C* **2015**, *119*, 13144. **Q9:** [APT to AU] Please check the presentation of author names in ref. 31 for correctness. [Reply by AU] corrected

32 S. I. Ahn, K. Kim, J. R. Jung, K. Y. Kang, S. M. Lee, J. Y. Han, K. C. Choi, *Chem. Phys. Lett.* **2015**, *625*, 36.

33 Z. Liu, S. P. Lau, F. Yan, *Chem. Soc. Rev.* **2015**, *44*, 5638.

34 S. Pei, H.-M. Cheng, *Carbon* **2012**, *50*, 3210.

35 N. Wei, C. Lv, Z. Xu, *Langmuir* **2014**, *30*, 3572.

36 H. Huang, Z. Song, N. Wei, L. Shi, Y. Mao, Y. Ying, L. Sun, Z. Xu, X. Peng, *Nat. Commun.* **2013**, *4*, 2979.

37 C. Z. Zhu, S. J. Gou, Y. X. Fang, S. J. Dong, *ACS Nano* **2010**, *4*, 2429. **Q10:** [APT to AU] Please check the presentation of author name 'S. Guo' in ref. 37 for correctness. [Reply by AU] corrected

38 O. Akhavan, E. Ghaderi, S. Aghayee, Y. Fereydooni, A. Talebi, *J. Mater. Chem.* **2012**, *22*, 13773.

39 F. Perrozzi, S. Croce, E. Treossi, V. Palermo, S. Santucci, G. Fioravanti, L. Ottaviano, *Carbon* **2014**, *77*, 473.

40 F. Bonaccorso, A. Lombardo, T. Hasan, Z. Sun, L. Colombo, A. C. Ferrari, *Mater. Today* **2012**, *15*, 564.

41 L. Sun, B. Fugetsu, *Mater. Lett.* **2013**, *109*, 207.

42 A. Giuri, S. Rella, C. Malitesta, S. Colella, A. Listorti, G. Gigli, A. Rizzo, P. D. Cozzoli, M. R. Acocella, G. Guerra, C. E. Corcione, *Sci. Adv. Mater.* **2015**, *7*, 2445.

43 M. Matsumoto, Y. Saito, C. Park, T. Fukushima, T. Aida, *Nat. Chem.* **2015**, *7*, 730. **Q11:** [APT to AU] Please check the presentation of author name 'Y. Saito' in ref. 43 for correctness. [Reply by AU] ok

44 Q. Luo, Y. Zhang, C. Liu, J. Li, N. Wang, H. Lin, *J. Mater. Chem. A* **2015**, *3*, 15996.

45 K. S. Novoselov, V. I. Fal'ko, L. Colombo, P. R. Gellert, M. G. Schwab, K. Kim, *Nature* **2012**, *490*, 192. **Q12:** [APT to AU] Please check the presentation of author name 'V. I. Fal'ko' in ref. 45 for correctness. [Reply by AU] ok

46 M. Hirata, T. Gotou, S. Horiuchi, M. Fujiwara, M. Ohba, *Carbon* **2004**, *42*, 2929.

47 F. Perrozzi, S. Prezioso, M. Donarelli, F. Bisti, P. De Marco, S. Santucci, M. Nardone, E. Treossi, V. Palermo, L. Ottaviano, *J. Phys. Chem. C* **2012**, *117*, 620.

48 W. Li, H. Dong, X. Guo, N. Li, J. Li, G. Niu, L. Wang, *J. Mater. Chem. A* **2014**, *2*, 20105.

49 C. Zhang, X. Peng, Z. Guo, C. Cai, Z. Chen, D. Wexler, S. Li, H. Liu, *Carbon* **2012**, *50*, 1897.

50 M. R. Acocella, M. Mauro, L. Falivene, L. Cavallo, G. Guerra, *ACS Catal.* **2014**, *4*, 492.

51 C. Wong, C. Lai, K. Lee, S. Hamid, *Materials* **2015**, *8*, 7118.

52 Y. Seekaew, S. Lokavee, D. Phokharatkul, A. Wisitsoraat, T. Kerdcharoen, C. Wongchoosuk, *Org. Electron.* **2014**, *15*, 2971.

53 Y. H. Ding, P. Zhang, Q. Zhuo, H. M. Ren, Z. M. Yang, Y. Jiang, *Nanotechnology* **2011**, *22*, 215601.

54 J. Li, C.-Y. Liu, Y. Liu, *J. Mater. Chem.* **2012**, *22*, 8426.

55 D. Alemu, H.-Y. Wei, K.-C. Ho, C.-W. Chu, *Energy Environ. Sci.* **2012**, *5*, 9662.

56 G. Greczynski, T. Kugler, M. Keil, W. Osikowicz, M. Fahlman, W. R. Salaneck, *J. Electron Spectrosc. Relat. Phenom.* **2001**, *121*, 1.

57 J. S. Stevens, S. L. M. Schroeder, *Surf. Interface Anal.* **2009**, *41*, 453.

58 S.-E. Chun, J. F. Whitacre, *Electrochim. Acta* **2012**, *60*, 392.

59 J. Zhou, D. H. Anjum, L. Chen, X. Xu, I. A. Ventura, L. Jiang, G. Lubineau, *J. Mater. Chem. C* **2014**, *2*, 9903.

60 Y. Xu, Y. Wang, J. Liang, Y. Huang, Y. Ma, X. Wan, Y. Chen, *Nano Res.* **2009**, *2*, 343.

61 A. Elschner, S. Kirchmeyer, W. Lovenich, U. Merker, K. Reuter, *PEDOT: Principles and Applications of an Intrinsically Conductive Polymer*, CRC Press, Taylor & Francis Group **2010**, 978-1-4200-6912-9, . **Q13:** [APT to AU] Please provide the publisher location in ref. 61. [Reply by AU] ok

62 K. Sun, Y. Xia, J. Ouyang, *Sol. Energy Mater. Sol. Cells* **2012**, *97*, 89.

63 S. Colella, E. Mosconi, G. Pellegrino, A. Alberti, V. L. Guerra, S. Masi, A. Listorti, A. Rizzo, G. G. Condorelli, F. De Angelis, G. Gigli, *J. Phys. Chem. Lett.* **2014**, *5*, 3532.

64 O. Malinkiewicz, A. Yella, Y. H. Lee, G. M. Espallargas, M. Graetzel, M. K. Nazeeruddin, H. J. Bolink, *Nat. Photonics* **2014**, *8*, 128.

65 Q. Lin, A. Armin, R. C. R. Nagiri, P. L. Burn, P. Meredith, *Nat. Photonics* **2015**, *9*, 106.

66 C. Roldán-Carmona, O. Malinkiewicz, R. Betancur, G. Longo, C. Momblona, F. Jaramillo, L. Camacho, H. J. Bolink, *Energy Environ. Sci.* **2014**, *7*, 2968.

67 L. K. Ono, S. Wang, Y. Kato, S. R. Raga, Y. Qi, *Energy Environ. Sci.* **2014**, *7*, 3989.

68 F. Fu, T. Feurer, T. Jäger, E. Avancini, B. Bissig, S. Yoon, S. Buecheler, A. N. Tiwari, *Nat. Commun.* **2015**, *6*, 8932.

69 C. O. R., Quiroz, I. Levchuk, C. Bronnbauer, M. Salvador, K. Forberich, T. Heumüller, Y. Hou, P. Schweizer, E. Spiecker, C. J. Brabec, *J. Mater. Chem. A* **2015**, *3*, 24071. **Q14:** [APT to AU] Please check the presentation of author names in ref. 69 for correctness. [Reply by AU] ok

70 D. Gaspera, E. Peng, Y. Hou, Q. Spiccia, L. Bach, U. J. J. Jasieniak, Y.-B. Cheng, *Nano Energy* **2015**, *13*, 249.

71 W. Chen, Y. Wu, J. Liu, C. Qin, X. Yang, A. Islam, Y.-B. Cheng, L. Han, *Energy Environ. Sci.* **2015**, *8*, 629.

72 L.-M. Chen, Z. Xu, Z. Hong, Y. Yang, *J. Mater. Chem.* **2010**, *20* , 2575.

73 N. K. Noel, A. Abate, S. D. Stranks, E. S. Parrott, V. M. Burlakov, A. Goriely, H. J. Snaith, *ACS Nano* **2014**, *8*, 9815.

74 C. J. Brabec, S. E. Shaheen, C. Winder, N. S. Sariciftci, P. Denk, *Appl. Phys. Lett.* **2002**, *80*, 1288.

75 C. D. Zangmeister, *Chem. Mater.* **2010**, *22*, 5625.

76 M. R. Acocella, C. E. Corcione, A. Giuri, M. Maggio, A. Maffezzoli, G. Guerra, *RSC Adv.* **2016**, *7*, 2445.

77 , A. Giuri, S. Masi, S. Colella, A. Listorti, A. Rizzo, G. Gigli, A. Liscio, S. Rella, C. Malitesta, E. TreossiV. PalermoC. Esposito Corcione, , *IEEE Trans. Nanotechnol.* **2016**, 10.1190/TNANO.2016.2524689.